IOP Publishing Journal of Physics D: Applied Physics
J. Phys. D: Appl. Phys. **49** (2016) 145103 (9pp) doi:10.1088/0022-3727/49/14/145103

High efficiency quantum dot and organic LEDs with a back-cavity and a high index substrate

Haowen Liang[1,2], Zhenyue Luo[1], Ruidong Zhu[1], Yajie Dong[1,4], Jiun-Haw Lee[5], Jianying Zhou[2,3] and Shin-Tson Wu[1]

[1] College of Optics and Photonics, University of Central Florida, Orlando, FL 32816, USA
[2] State Key Laboratory of Optoelectronic Materials and Technologies, Sun Yat-sen University, Guangzhou 510275, People's Republic of China
[3] SYSU-CMU Shunde International Joint Research Institute, Shunde 528300, People's Republic of China
[4] NanoScience Technology Center, University of Central Florida, Orlando, FL 32816, USA
[5] Graduate Institute of Photonics and Optoelectronics and Department of Electrical Engineering, National Taiwan University, Taipei 10617, Taiwan

E-mail: swu@ucf.edu

Received 6 August 2015, revised 29 January 2016
Accepted for publication 9 February 2016
Published 10 March 2016

Abstract

We report a back-cavity design to enhance the optical efficiency of a quantum dot light-emitting diode (QLED) or an organic light-emitting diode (OLED) for display and lighting applications. Our simulation results show that the back-cavity design exhibits two major advantages: (1) the transparent electrode helps to increase the transmittance of backward light despite using a semi-transparent metal electrode, and (2) the thickness of the low index optical buffer layer can be optimized to modify the proportion of each optical channel. The proposed back-cavity also helps to lower the refractive index of the high-index substrate from ~2.0 to ~1.8 for achieving high optical efficiency. Finally, the introduced back-cavity does not degrade the color performance of the QLED/OLED.

Keywords: quantum dot display, light emitting diode, thin film device

(Some figures may appear in colour only in the online journal)

1. Introduction

Colloid quantum dots light-emitting diodes (QLEDs) have attracted increasing attention for next generation display and lighting applications [1–6] due to their saturated colors, tunability of emission spectra through particle size control and high photoluminescence (PL) quantum efficiency. The internal quantum efficiency (IQE) of a QLED can reach nearly 100% [1, 3, 4, 6, 7] but only ~20% of external quantum efficiency (EQE) is achieved without any additional light extraction assistance [8]. The remaining 80% power is trapped in the substrate and organic/inorganic hybrid layers, or evanesces at the surface of metal electrode [9]. Therefore, enhancing the outcoupling efficiency is urgently needed in order to reduce power consumption and extend the device lifetime.

Considering the similarity between QLED and organic light-emitting diode (OLED), various photonic structures implemented in OLEDs for increasing EQE can also be introduced to QLEDs, such as low-index dielectric grid [10, 11], subwavelength photonic crystals [12–14], microlens arrays [15–17], random/quasi-random buckles [18] or periodic metallic grating electrode [19–21]. Among these light extraction strategies, microlens arrays (external extractor) can just extract the substrate mode; while other internal extractors are capable to dig out the waveguide mode from devices, which is considered to further increase the outcoupling efficiency. The latter ones are attracting great interest from both academia and industry, but they are not yet ready for mass production.

Recently high index substrates are reported to have potential applications because the waveguide mode in an QLED/

OLED can be totally cancelled if the refractive index of substrate (n_{sub}) is larger than the equivalent refractive index (n_{eff}) of the organic layer, QD layer and indium tin oxide (ITO) [22, 23]. It is reported that ~80% power can be extracted with a high index substrate and microextractors without the need of any internal extraction structure. This value is obtained at the second field antinode in order to suppress the surface plasmonic loss [31]; however, the thickness of hole transport layer (HTL) at second field antinode is rather large (more than 100 nm). As a result, holes are more likely to recombine within the HTL, which degrades the transporting ability of the HTL [24, 25]. It is meaningful to study how to recycle the dissipated power without degrading the electrical characteristic of the device.

In this paper, we propose a scheme of bottom emission QLED/OLED with a back-cavity. The back-cavity consists of an ITO transparent electrode layer, an optical buffer layer (OBL) and a metal mirror layer. By engineering the OBL thickness, the HTL thickness remains at first field antinode while we can get similar results as at the second field antinode. The metal mirror reflects light back to the air and the substrate. By inserting a high index substrate, over 87% of light distributes in both air and substrate and the waveguide mode can be totally cancelled. Finally, lens technique is applied to further extract light from substrate into air. The whole structure is compatible to the industrial manufacturing process, and it has potential to be implemented in both display and lighting devices.

2. Theoretical model

To verify our design, a reliable theoretical model should be built up at first. As the outcoulping efficiency of the device is the major concern, here we use the rigorous dipole model because it can provide complete information in irradiance spectra, outcoupling efficiency, and angular dependence [8, 9, 19, 24]. In the dipole model, the emission sources of QLED/OLED is assumed to be isotropic dipole emitters within a multilayer medium. The refractive indices of each layer in our models are taken from [28, 32], that have been verified experimentally and widely accepted. Here we would like to clarify that this theoretical model is applicable to normal OLED/QLED analysis for the following reasons: (1) the refractive indices of organic materials in a QLED/OLED are similar ($n_{org} \approx 1.6$–1.8); (2) the length of micro-cavity in normal QLEDs/OLEDs is about $\lambda/4$; 3) the layers in both forward structure and inverted structure of QLEDs/OLEDs have similar optical properties. According to these features, the typical devices used here are representative for mode analysis.

A bottom emitted red QLED structure [1, 6] consists of layers depicted in figure 1(a): ITO/ZnO nano-particle (40 nm)/ Hole blocking layer (~10 nm)/CdSe–ZnS–CdZnS QD monolayer (9 nm)/2,2′,7,7′-tetrakis [N-naphthalenyl(phenyl)-amino]-9,9-spirobifluorene (spiro-2NPB, 65 nm)/ dipyrazino [2,3-f:20,30-h]quinozaline-2,3,6,7,10,11-hexacarbonitrile (HAT-CN, 15 nm)/ Aluminum 100 nm. The PL spectrum of the reported QDs is shown in figure 1(c). The central wavelength is 615 nm with FWHM ~ 22 nm, quantum yield ~ 100%, and outstanding optical properties [1, 6].

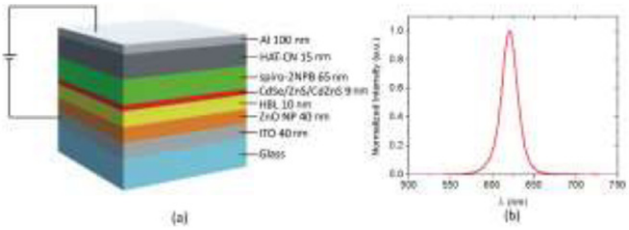

Figure 1. (a) The QLED structure and (b) PL spectrum of the CdSe/ZnS/CdZnS QD reported in [6]. The central wavelength is 615 nm with FWHM ~ 22 nm and quantum yield ~ 100%.

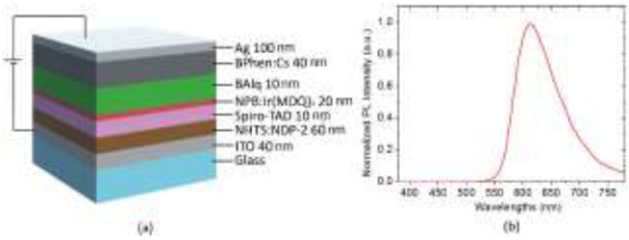

Figure 2. (a) A typical red OLED structure and (b) the PL spectrum of NPB:Ir(MDQ)$_2$ (acetylacetonate).

For a benchmark, we use a red OLED structure as figure 2 shows: ITO/NHT-5: NPD-2 (60 nm)/spiro-TAD (10 nm)/ NPB:Ir(MDQ)$_2$ (acetylacetonate) (20 nm)/BAlq (10 nm)/ BPhen:Cs (40 nm)/Ag (100 nm). A profound analysis of this structure has been reported in [28].

The EQE of the QLED/OLED is described as:

$$\mathrm{EQE} = \eta \mathrm{IQE}, \tag{1}$$

where η is the outcoupling efficiency of the planar QLED/OLED structure and IQE is the IQE. The quantum efficiency is tightly related to the quantum yield of QDs [8, 9, 22, 24]. As quantum yield is approaching 100% [1, 6], the IQE is approximated to 1 in this study (also the IQE of the OLED can be approximated to 1).

The dipole model can give quantitative power dissipation results of a QLED/OLED [9, 26]. In the dipole model, both transverse magnetic (TM) and transverse electric (TE) waves are taken into consideration. The power dissipation density K can be calculated for randomly oriented dipoles as:

$$K = \frac{1}{3}K_{\mathrm{TM}v} + \frac{2}{3}(K_{\mathrm{TM}h} + K_{\mathrm{TE}h}), \tag{2}$$

where $K_{\mathrm{TM}v}$ denotes for vertical dipoles coupling to TM waves ($K_{\mathrm{TE}v} = 0$ for vertical dipoles coupling to TE waves), and $K_{\mathrm{TM}h}$ and $K_{\mathrm{TE}h}$ for horizontal dipoles coupling to TM and TE waves, respectively. The detailed description of each term in equation (2) can be found in [22].

To analyze the optical modes in a QLED/OLED, we assume the device is working at a stable state, which means the interaction between modes is balanced. As a result, the mode variation can be ignored [9, 24] and the optical modes of a typical QLED/OLED can be sorted out by the in-plane wave vector k_x [31]: (1) direct emission (air mode), depicting the light directly emitting into air when $0 < k_x \leqslant k_0 \cdot n_{\mathrm{air}}$ ($k_0 = 2\pi/\lambda$ is the vacuum wave vector); (2) substrate mode, showing light trapped in substrate due to total internal reflection (TIR) when

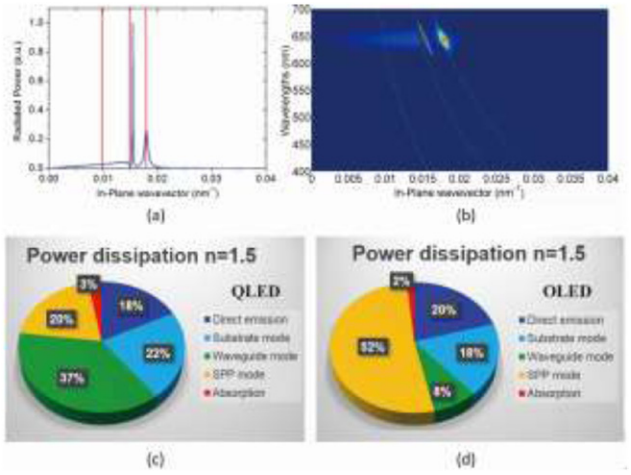

Figure 3. The optical performance of our proposed QLED: (a) power dissipation spectra at 640 nm and (b) full dissipation power spectra. The ratios of different optical channels of (c) a QLED and (d) an OLED.

$k_0 \cdot n_{\text{air}} < k_x \leqslant k_0 \cdot n_{\text{sub}}$ ($k_0 = 2\pi/\lambda$ is the vacuum wave vector); (3) waveguide mode, showing light guided inside the organic/inorganic hybrid layers because of TIR at the ITO/glass interface when $k_0 \cdot n_{\text{sub}} < k_x \leqslant k_0 \cdot n_{\text{eff}}$. n_{eff} is the real part of the equivalent refractive index of the organic/inorganic hybrid layers and ITO layer. It can be expressed as:

$$\varepsilon_{\text{eff}} = \sum_i d_i / \sum_i (d_i/\varepsilon_i),$$
$$n_{\text{eff}} = \text{Re}\left(\sqrt{\varepsilon_{\text{eff}}}\right). \tag{3}$$

In equation (3), d_i is the layer thickness, ε_i is the corresponding dielectric constant, and ε_{eff} is the equivalent dielectric constant. (4) Surface plasmon polaritons (SPPs) mode: this mode corresponds to the evanescent wave at the organic/metal interface, where $k_0 \cdot n_{\text{eff}} \leqslant k_x$. Notice that waveguide mode can be eliminated if $n_{\text{eff}} \leqslant n_{\text{sub}}$. With equations (1) and (2) the power dissipation P_{tol} through the entire visible spectrum (from $\lambda_1 = 380$ nm to $\lambda_2 = 780$ nm) and the EQE can be given as:

$$P_{\text{tol}} = 1 - q + q \int_{\lambda_1}^{\lambda_2} S(\lambda) \int_0^{\infty} K(k_x) \mathrm{d}k_x \mathrm{d}\lambda, \tag{4}$$

$$\text{EQE} = P_{\text{air}}/P_{\text{tol}}, \tag{5}$$

where q is the intrinsic quantum yield of the QDs or NPB:Ir(MDQ)$_2$ (acetylacetonate), $S(\lambda)$ is the PL spectrum depicted in figure 1(b) or figure 2(b), and P_{air} is the power of direct emission.

Figures 3(a) and (b) show the simulation results for the power dissipation of a typical QLED. In figure 3(c), the EQE of a typical QLED structure is 18%. Our simulated results match well with those reported in [1]. Most of the light is trapped in substrate mode and waveguide mode. This amount of light can be extracted by either internal or external extraction strategies. However, 20% of the power dissipating in SPP mode and 3% due to absorption cannot be extracted via any extraction methods. Similar analysis is conducted on the red

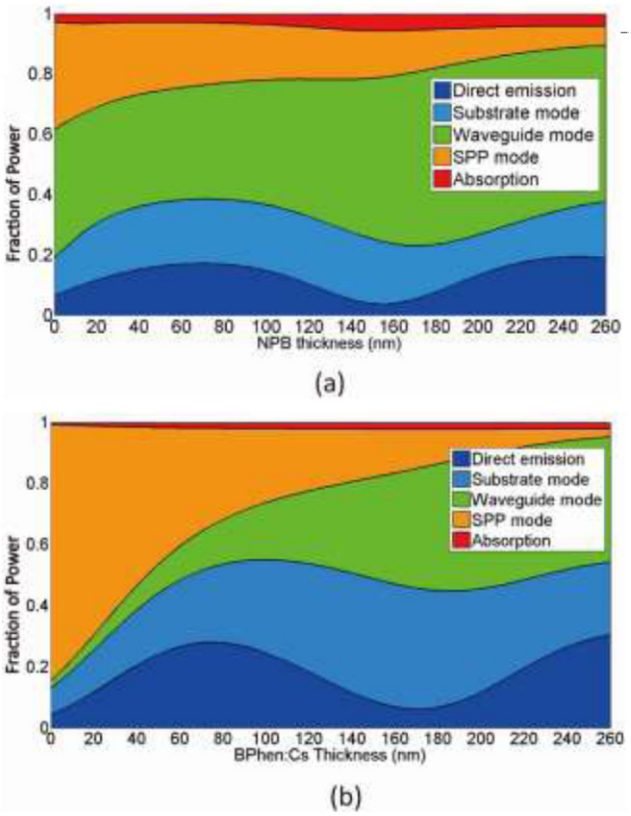

Figure 4. Changing the proportions of different optical channels by (a) tuning the thickness of NPB in an QLED and (b) tuning the thickness of BPhen:Cs in an OLED.

OLED. Figure 3(d) shows that SPP mode is even larger in an OLED than in a QLED.

A straightforward way to optimize the power distribution is to engineer the thickness of HTL (spiro-2NPB) in a QLED [24, 31]. The distance from the emitting layer to the metallic electrode mainly determines the coupling to SPP. SPP is mitigated with an increasing HTL thickness. The optimal thickness of HTL is at 75 nm (first field antinode) with 18% direct emitting power and 247 nm (second field antinode) with 19% direct emitting power respectively. At the second field antinode the SPP mode is suppressed with a thicker HTL layer. Meanwhile, the variation of HTL thickness greatly modifies the QLED cavity, as can be seen in the direct emission part. These results are clearly shown in figure 4.

To enhance the EQE of QLED/OLED, high index substrates are helpful to further confine power in the substrates. With higher index, the waveguide mode can be totally eliminated and the SPP mode is further suppressed. With an increasing thickness of NPB (BPhen:Cs for the OLED case), the equivalent index (n_{eff}) of the organic layers approaches to the index of NPB ($n_{\text{NPB}} \approx 1.9$) or BPhen:Cs ($n_{\text{BPhen:Cs}} \approx 1.8$). As a result the index of substrate should be higher than the equivalent index of to convert the waveguide mode into substrate mode.

3. Simulation on back-cavity design

As explained above, by optimizing the HTL thickness, using a high index substrate and outcoupling techniques, the EQE

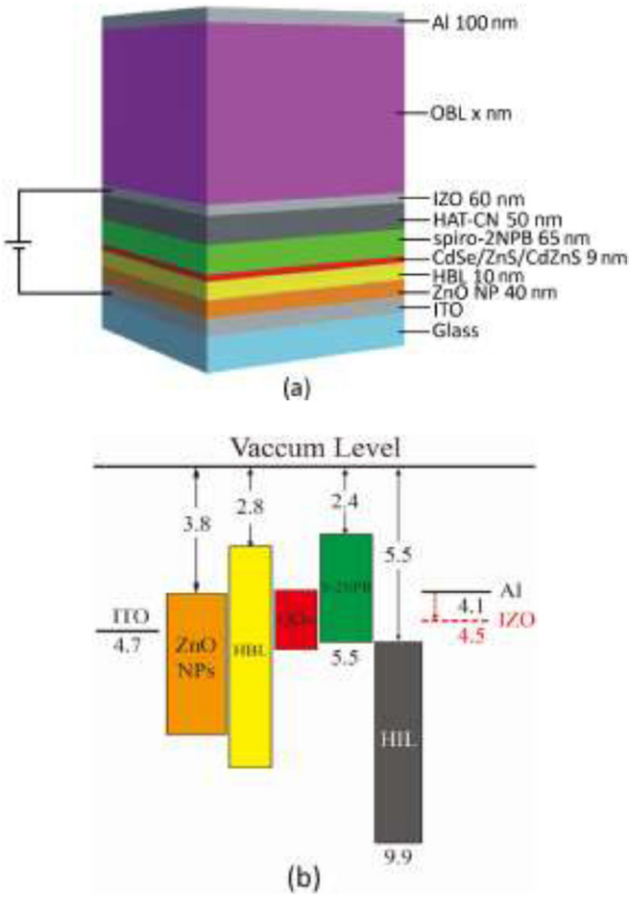

Figure 5. (a) Schematic device structure and (b) energy band diagram of the proposed QLED with a back-cavity. Even though IZO has a higher energy level than Al, the carriers can still be injected in the device due to the low LUMO level of HAT-CN.

of a QLED/OLED can be improved significantly without applying any internal extraction strategies (e.g. photonic crystal, random buckles, etc). However, this approach has tradeoffs in the following two aspects: (1) such a high index substrate is expensive, heavy and hazing to eyes; (2) the electrical property of a thick HTL could deteriorate. To modify the HTL thickness, it either needs to be electrically doped or have a very high charge conductivity to assure that Ohmic losses and changes of charge carrier balance can be excluded [24]. Although the theoretical prediction of direct emission can reach as high as 19% from the optics viewpoint, it is difficult to achieve the second field antinode. A thick HTL leads to an electric field redistribution in the whole device; therefore carriers are more likely to recombine within the HTL, which consequently results in a negative impact on the injection and transport process of both carriers [25].

To address the above problems, here we propose a design to reach second field antinode by embedding a back-cavity to avoid electrical doping in the HTL. The back-cavity consists of an OBL and a reflective metal electrode (shown in figure 5(a)). Inspired by the transparent OLEDs, the metal top contact is replaced by ITO or indium zinc oxide (IZO) layer with 60 nm. IZO is a promising transparent electrode candidate because of its low work function (≈4.5 eV), high transparency (~80%), low resistivity and low surface roughness.

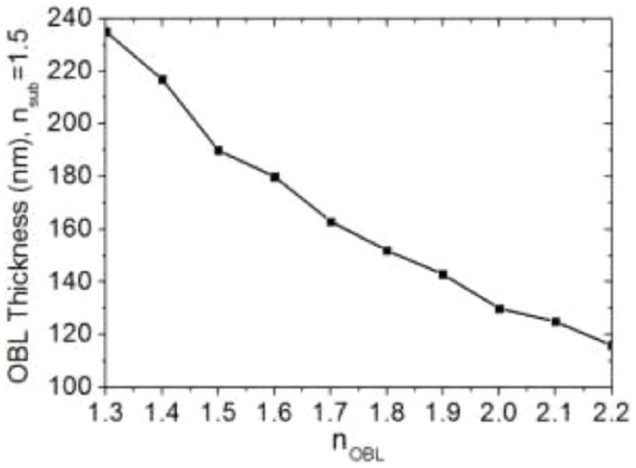

Figure 6. Interrelation between refractive index of substrate (n_{OBL}) and thickness of OBL.

Meanwhile, HAT-CN provides two positive aspects to our structure: (1) it possesses a deep lowest unoccupied molecular orbital (LUMO), as shown in figure 5(b). Therefore with ITO or IZO the holes can still be easily injected into the device; (2) it is reported that HAT-CN effectively protects the underlying organic emission layer from damage caused by sputter deposition of IZO or ITO [29, 30]. Here the thickness of HAT-CN increases to 50 nm compared to our proposed QLED. This approach does not degrade the electrical property of HAT-CN because of its good hole injection performance. Similar arguments also hold for OLED.

The OBL is made of total dielectric to separate the top transparent electrode and the reflective metal electrode. Equation (3) denotes that modifying the thickness of OBL contributes to the equivalent refractive index, giving rise to the cavity modification similar to the effect in figure 4. Figure 6 shows the interrelation between refractive index n_{OBL} and thickness of the OBL. Generally, the thickness decreases while choosing the OBL with a higher n_{OBL}. In order to match the refractive index of substrate n_{sub}, in this case, a refractive index of $n_{OBL} \approx 1.48$ (a highly transparent dielectric material, e.g. SiO_2) is chosen. Figure 7(a) illustrates the simulated cavity modification effect of the QLED incorporating our back-cavity design. When the OBL thickness is 187 nm, we can achieve 38% of power if we consider both direct emission (20.6%) and substrate mode (17%). For an OLED (figure 7(b)), the effects are more significant (26.2% in direct emission and 22.1% in substrate mode) with the OBL thickness of 230 nm. We also compare the case of OBL with a higher refractive index $n_{OBL} \approx 1.8$ (e.g. α-NPD, NPB, *m*-MTDATA) in figures 7(c) and (d).

As the OBL thickness increases, the equivalent index of the device approaches to that of OBL. For OBL with a high index such that $n_{eff} > n_{sub}$, the SPP mode can be mitigated with a thicker OBL; while the SPP mode increases with a low index OBL because the transmissive light evanesces at the surface of the reflective metal electrode. Thus, a large portion of the trapped light is converted to SPP mode rather than waveguide mode. This part of light cannot be utilized by any of the extraction strategies.

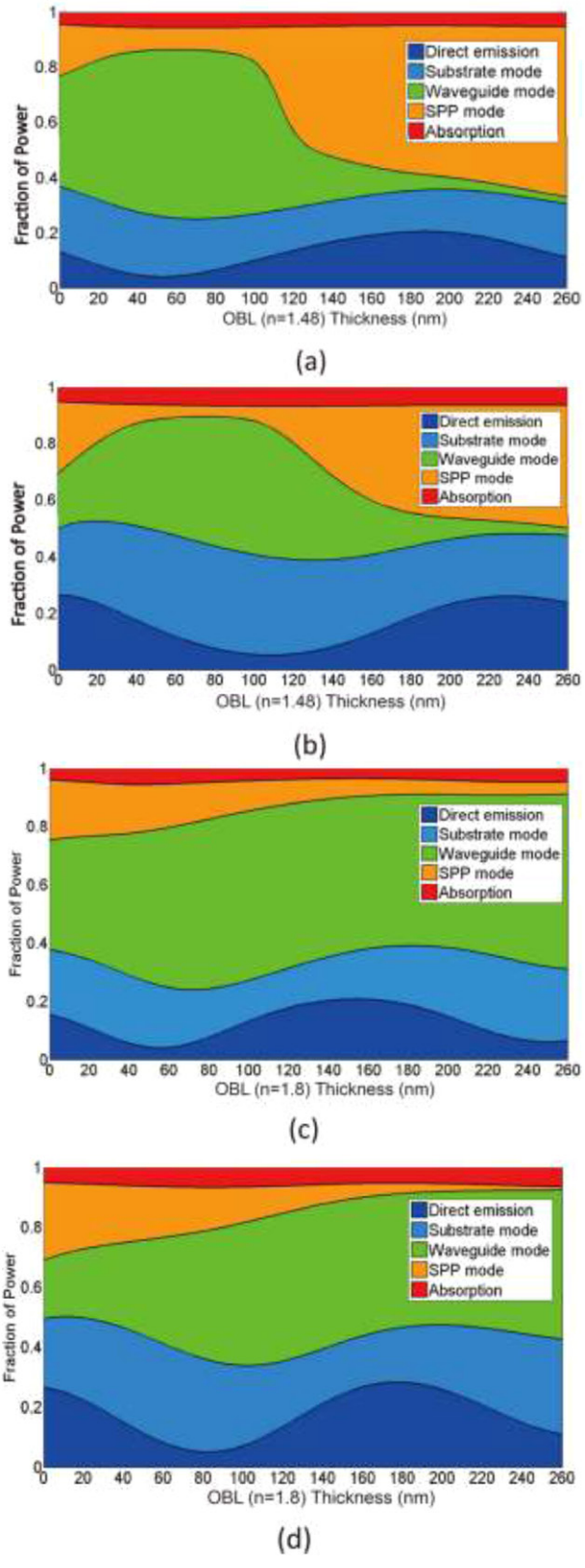

Figure 7. Changing the proportions of different optical channels by tuning the OBL thickness with $n_{sub} = 1.5$ substrate for QLED: (a) $n_{OBL} = 1.48$ and (c) $n_{OBL} = 1.8$, and for OLED: (b) $n_{OBL} = 1.48$ and (d) $n_{OBL} = 1.8$.

Another bottleneck is that most of the light is trapped in waveguide mode due to TIR, which is a result of the large refractive index mismatch between glass substrate ($n_{sub} \approx 1.5$),

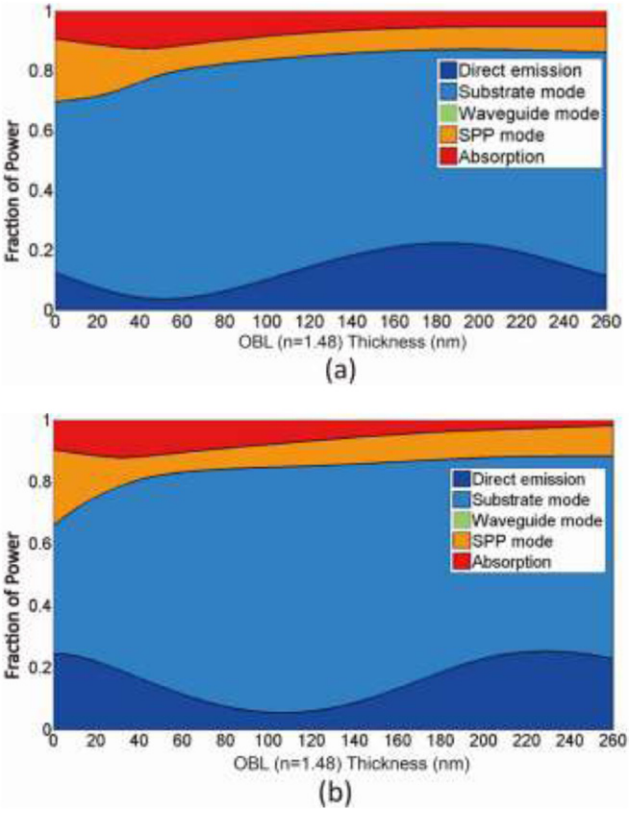

Figure 8. Changing the proportions of different optical channels by tuning the thickness of OBL with $n_{OBL} = 1.48$ substrate in (a) QLED and (b) OLED.

organic layers ($n_{org} \approx 1.6$–1.8) and ITO ($n_{ITO} \approx 1.8$). To suppress the waveguide mode, a high index substrate ($n_{sub} \approx 1.8$–2.0) should be introduced in order to guide the wave towards the substrate. High index substrate is made of metal-doped (e.g. Ba^{4+}, La^{3+}) glass. It is reported that $n_g \approx 2.0$ is optimal for the substrates [22]. With such a high index substrate, ~80% of the total power in an QLED/OLED can be extracted by using outcoupling structures, which is ~2X improvement compared to that of using a low index BK7 glass ($n_{sub} \approx 1.5$), if we count both direct emission and substrate modes. However, glass substrate with $n_g \approx 2.0$ is expensive and still difficult to manufacture. Lowering the substrate refractive index, e.g. $n_{sub} \approx 1.8$, is an important step to increase the efficiency of the device.

As discussed above, the light tends to distribute in the high index layers. Thus, a high index substrate offers a better match between glass and ITO. Meanwhile, the low index OBL helps to lower the effective index of the organic stacks, which can further boost the energy to bottom side of the device. Therefore, a low index OBL is index advantageous when a high index substrate is used.

Figure 8 illustrates the simulated power dissipation distribution with a high index substrate ($n_{sub} \approx 1.80$, N-LAF21, SCHOTT). At the same OBL ($n_{OBL} = 1.48$) thickness of 187 nm, the direct emission part increases to 22.5% and totally 87.5% of power is guided into both air mode and substrate mode. It is about 10% higher than the maximum value of an original QLED with an $n_{sub} = 2.0$ (P-SF68, SCHOTT)

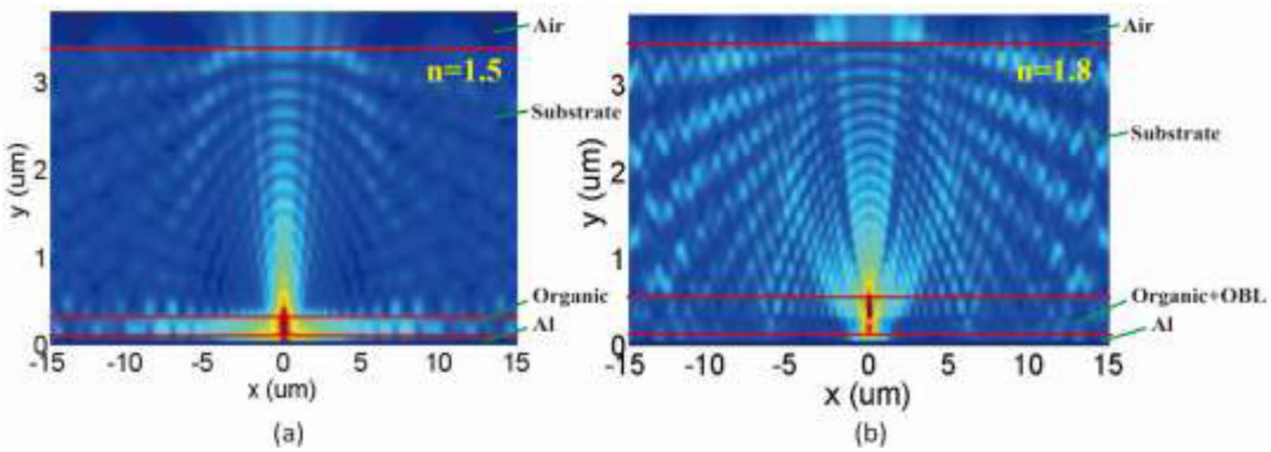

Figure 9. FDTD simulation results showing (a) light trapped within the device with $n_{sub} = 1.5$ substrate and (b) with $n_{sub} = 1.8$ substrate and OBL combination.

Table 1. Fractions of power coupled to different modes for QLEDs with substrates with various refractive index.

	Substrate	Direct emission	Substrate mode	Waveguide mode	SPP mode	Absorption
w/o OBL [22]	$n_{sub} = 1.5$	19.2%	19.4%	36.1%	22.0%	3.2%
	$n_{sub} = 1.7$	19.2%	40.5%	8.7%	26%	5.6%
	$n_{sub} = 1.8$	19.2%	43.6%	4.3%	26.9%	6.0%
	$n_{sub} = 2.0$	19.0%	59.3%	0.0%	5.6%	16.1%
	$n_{sub} = 2.2$	18.7%	62.0%	0.0%	2.4%	16.9%
	$n_{sub} = 2.4$	18.3%	62.6%	0.0%	1.6%	17.5%
w/OBL ($n_{OBL} = 1.48$)	$n_{sub} = 1.5$	20.6%	15.0%	5.7%	53.9%	4.8%
	$n_{sub} = 1.7$	21.9%	33.1%	0.0%	38.0%	7.0%
	$n_{sub} = 1.8$	22.5%	64.8%	0.0%	3.1%	9.5%
	$n_{sub} = 2.0$	22.3%	65.2%	0.0%	2.8%	9.7%
	$n_{sub} = 2.2$	22.0%	65.5%	0.0%	2.3%	10.2%
	$n_{sub} = 2.4$	21.8%	65.8%	0.0%	1.9%	10.5%
w/OBL ($n_{OBL} = 1.8$)	$n_{sub} = 1.5$	20.6%	17.6%	52.4%	5.8%	3.6%
	$n_{sub} = 1.7$	22.0%	36.0%	28.3%	6.4%	7.3%
	$n_{sub} = 1.8$	22.7%	57.1%	2.2%	7.5%	10.4%
	$n_{sub} = 2.0$	22.5%	57.5%	0.0%	1.6%	18.4%
	$n_{sub} = 2.2$	21.7%	57.9%	0.0%	1.3%	19.1%
	$n_{sub} = 2.4$	21.3%	57.6%	0.0%	1.1%	20.0%

substrate. If we count both direct emission and substrate mode, the modified QLED and OLED possess almost the same optical efficiency distribution because of the OBL and the high index substrate. In figure 9, we compare the simulated light performance of our proposed QLED/OLED with $n_{sub} = 1.5$ substrate (figure 9(a)) and that with OBL and $n_{sub} = 1.8$ substrate (figure 9(b)). From figure 9(b), we find that high index substrate helps extract light into both air and substrate; SPP mode is suppressed because a large amount of light is guided into the high index substrate; and finally the waveguide mode is cancelled because of the OBL. The FDTD results validate our model design.

Table 1 lists the fractions of power coupled to different modes for a QLED/OLED with substrates of various refractive index. Similar results are given compared to the proposed results in [22]. High index substrates help suppress the waveguide mode as the refractive index of the substrate increases. After the waveguide mode is totally eliminated, absorption dominates the proportion of trapped light and the light extracted to direct emission and substrate mode gradually saturates. However, cost and weight of a substrate increases with higher index. A major advantage of OBL with low refractive index ($n_{OBL} = 1.48$) is to lower the optimal index of the substrate from $n_{sub} = 2.0$ (without OBL) to $n_{sub} = 1.8$. From figure 10, we also find that a nearly 30% gain is achieved with OBL compared to that without OBL if we consider the refractive index of substrates is $n_{sub} = 1.8$ in both cases.

4. Analysis of emission pattern

For display applications, the angular emission properties of the device affect the viewing angle and color shift. For a typical QLED, its angular emission pattern is Lambertian, as figure 11(a) shows. While for our proposed QLED with a high

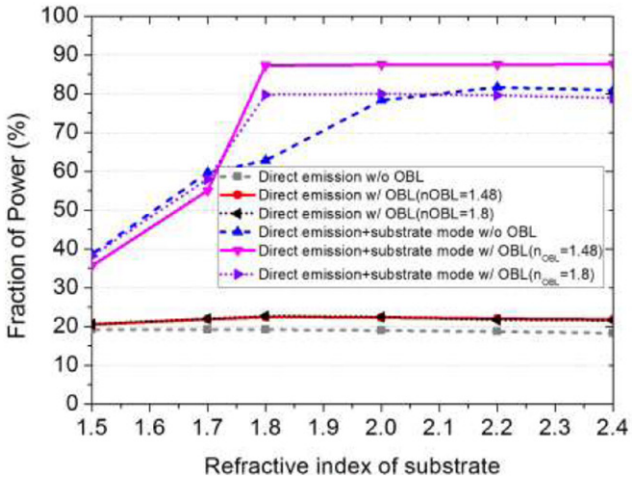

Figure 10. The power proportion of a QLED and a QLED+OBL with different refractive index.

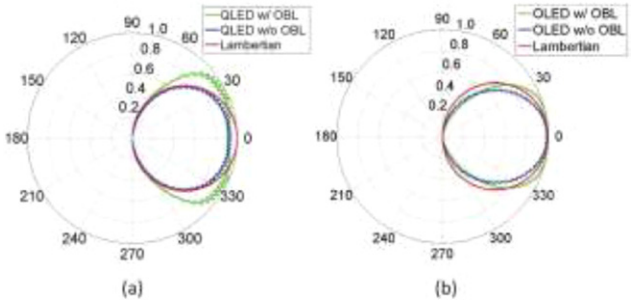

Figure 11. Angular emission pattern of (a) a QLED and (b) an OLED with and without OBL.

index substrate and an OBL, its emission intensity is higher at the two side views (around $\pm 30°$) because the back-cavity changes the micro-cavity effect of the device. The stronger side light is induced due to the reflection from the Al mirror. While side light is induced with an OBL, the viewing angle is preserved to be around $\pm 60°$ in both cases. For an OLED (figure 11(b)), we can obtain similar results, but the gain of the emission part from the back-cavity is not as large as that of QLED because of its wider FWHM.

To characterize the color performance of a display device, first of all we analyze the EL spectrum from different viewing angles. Color shift occurs because of the inhomogeneous broadening of the spectrum from different viewing angles. Figure 12(a) illustrates the simulated emission spectrums of our proposed QLED. As the FWHM of the QLED EL spectrum is very narrow, the inhomogeneous broadening of the red QLED is hardly noticeable. For a QLED with an OBL, the emission intensity increases as the angle changes from $10°$ ($-10°$) to $30°$ ($-30°$), and then decreases (figure 12(b)). However, the emission spectrum of an OLED is sensitive to the thickness of the micro-cavity. The inhomogeneous broadening is noticeable for OLED because its emission spectrum is much broader than that of QDs.

Figure 12(c) shows the emission spectrum of a typical OLED and figure 12(d) indicates that the back-cavity significantly increases the inhomogeneous broadening in the OLED. Moreover, a blue shift is observed at the oblique angles. These

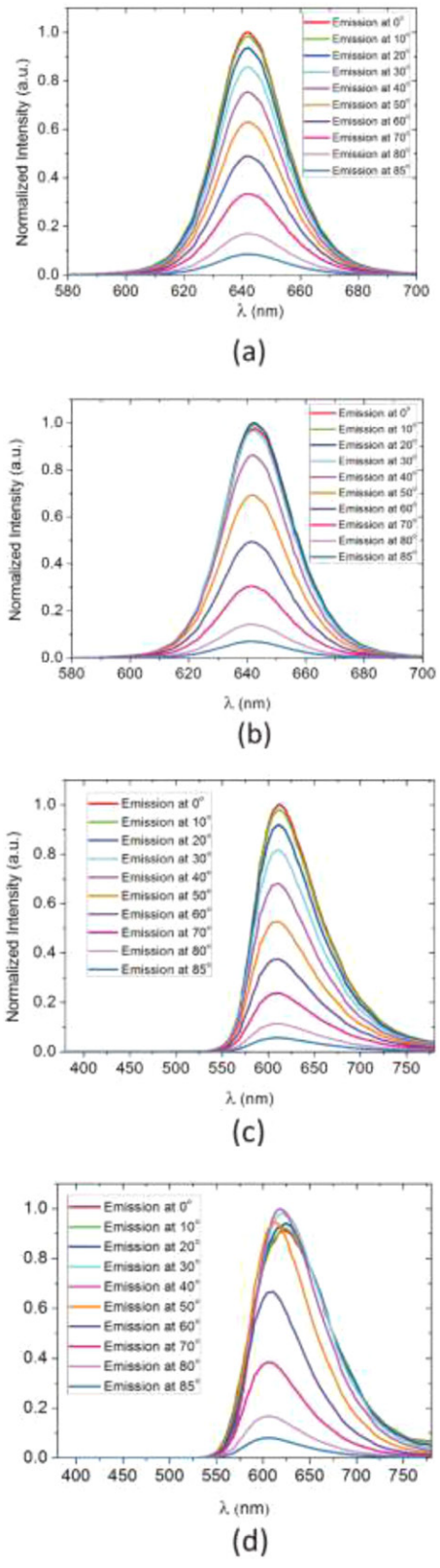

Figure 12. EL spectra of a QLED (a) without and (b) with OBL, and EL spectra of an OLED (c) without and (d) with OBL.

results coincide with the illustration in figure 11, and it indicates that an OBL increases the color shift of both QLED and OLED.

Figure 13(a) depicts the color shift of our red QLED. The simulated $\Delta u'v'$ value is smaller than 0.002, indicating that

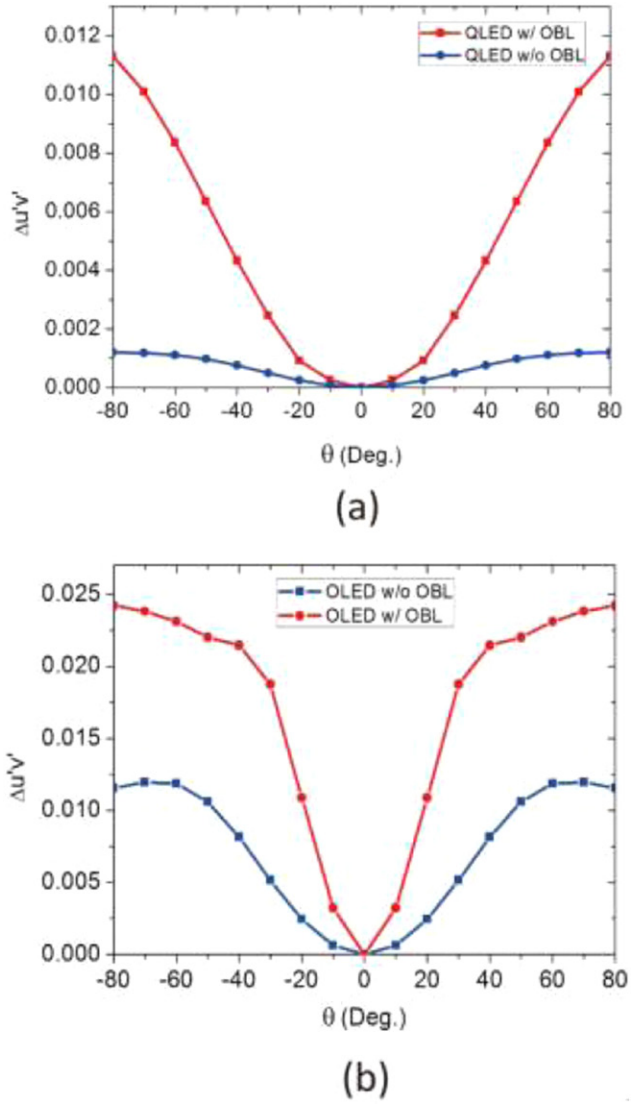

Figure 13. Simulated color shift of the proposed red (a) QLED and (b) OLED with and without OBL.

the color shift remains unnoticeable even at a large oblique angle. However, with OBL the $\Delta u'v'$ jumps to ~0.01 because the OBL changes the micro-cavity length of the device. Fortunately, the FWHM of the QLED is so narrow that this color shift is still indistinguishable to human eye (<0.02) and it is comparable to the value of the OLED [22]. This result coincides with the benefit of quantum-dots-enhanced LCDs to mitigate color shift [27]. We expect that similar results can be obtained for green and blue QLEDs. Therefore, the proposed OBL structure still keeps color shift in the unnoticeable range.

For the red OLED with OBL, its color shift is an issue. The $\Delta u'v'$ value of our originally proposed OLED is ~0.012 because of its broad FWHM. However, inhomogeneous broadening from the back-cavity dramatically increases the $\Delta u'v'$ value to above ~0.02 (figure 13(b)), which makes the color shift noticeable to human eye. To mitigate the inhomogeneous broadening of an OLED, we should reduce the OBL thickness. However, the direct emission part drops if the OBL thickness deviates from the second field antinode, according to figure 8(b). Fortunately, most of the dissipated power is guided into substrate mode because of the high index of the substrate and this part of power can be extracted via microlens. Therefore, a thinner OBL does not sacrifice too much on the power, while lessening color shift.

5. Summary

Our simulated results of the proposed QLED/OLED with a back-cavity and a high index substrate can effectively enhance the optical efficiency if both direct emission and substrate mode are counted. By optimizing the thickness of the low refractive index OBL, the micro-cavity of the QLED/OLED is modified to the second antinode while the electrical property of HTL does not degrade. To cancel the waveguide mode and further reduce the SPP mode, a high index substrate is applied to redistribute the power proportion. It is shown that a high index substrate with an OBL extracts almost 90% of the power to both direct emission and substrate modes. Moreover, there is a 40% efficiency gain for the QLED with the OBL and $n_{sub} = 1.8$ substrate combination compared to the QLED with barely $n_{sub} = 1.8$ substrate. For the red QLED, although the OBL increases color shift, its $\Delta u'v'$ value is still in the acceptable range. However, the OBL dramatically increases the $\Delta u'v'$ value of an OLED to above 0.02. This problem can be lessened by using a thinner OBL, while the efficiency can be preserved via high index substrate and microlens extraction method. Thus, we confirm that our simulated results of the back-cavity is a guidance and approach for high efficiency QLED/OLED displays.

Acknowledgment

H Liang is indebted to the financial support from 2014 International Program for PhD candidates, Sun Yat-sen University, Guangzhou, China and Pilot Project of SYSU-CMU Shunde International Joint Research Institute (20150101).

References

[1] Mashford B S *et al* 2013 *Nat. Photon.* **7** 407
[2] Qian L, Zheng Y, Xue J and Holloway P H 2011 *Nat. Photon.* **5** 543
[3] Dai X, Zhang Z, Jin Y, Niu Y, Cao H, Liang X, Chen L, Wang J and Peng X 2014 *Nature* **515** 96
[4] Yang Y, Zheng Y, Cao W, Titov A, Hyvonen J, Manders J R, Xue J, Holloway P H and Qian L 2015 *Nat. Photon.* **9** 259
[5] Kwak J *et al* 2012 *Nano Lett.* **12** 2362
[6] Dong Y *et al* 2015 *SID Symp. Dig. Tech. Pap.* **46** 270
[7] Shen H, Bai X, Wang A, Wang H, Qian L, Yang Y, Titove A, Hyvonen J, Zheng Y and Li L 2014 *Adv. Funct. Mater.* **24** 2367
[8] Meerheim R, Furno M, Hofmann S, Lüssem B and Leo K 2010 *Appl. Phys. Lett.* **97** 253305
[9] Brütting W, Frischeisen J, Schmidt T D, Scholz B J and Mayr C 2013 *Phys. Status Solidi* a **210** 44
[10] Sun Y and Forrest S R 2008 *Nat. Photon.* **2** 483
[11] Koh T W, Choi J M, Lee S and Yoo S 2010 *Adv. Mater.* **22** 1849
[12] Lee Y, Kim S, Huh J, Kim G, Lee Y, Cho S, Kim Y and Do Y 2003 *Appl. Phys. Lett.* **82** 3779

[13] Yang X *et al Adv. Funct. Mater.* **24** 5977
[14] Liang H, Zhu R, Dong Y, Wu S T, Li J, Wang J and Zhou J 2015 *Opt. Express* **23** 12910
[15] Möller S and Forrest S R 2002 *J. Appl. Phys.* **91** 3324
[16] Wei M K and Su I L 2004 *Opt. Express* **12** 5777
[17] Yang J, Bao Q, Xu Z, Li Y, Tang J and Shen S 2010 *Appl. Phys. Lett.* **97** 223303
[18] Koo W H, Jeong S M, Araoka F, Ishikawa K, Nishimura S, Toyooka T and Takezoe H 2010 *Nat. Photon.* **4** 222
[19] Oskooi A 2015 *Appl. Phys. Lett.* **106** 041111
[20] Feng J, Okamoto T and Kawata S 2005 *Opt. Lett.* **30** 2302
[21] Hauss J, Bocksrocker T, Riedel B, Geyer U, Lemmer U and Gerken M 2011 *Appl. Phys. Lett.* **99** 103303
[22] Zhu R, Luo Z and Wu S T 2014 *Opt. Express* **22** A1783
[23] Reineke S, Lindner F, Schwartz G, Seidler N, Walzer K, Lüssem B and Leo K 2011 *Nature* **459** 234
[24] Reineke S, Thomschke M, Lüssem B and Leo K 2013 *Rev. Mod. Phys.* **85** 1245
[25] Zhou Y, Zhou J, Zhao J, Zhang S, Zhan Y, Wang X, Wu Y, Ding X and Hou X 2006 *Appl. Phys.* A **83** 465
[26] Neyts K A 1998 *J. Opt. Soc. Am.* A **15** 962
[27] Luo Z, Xu D and Wu S T 2014 *J. Disp. Technol.* **10** 526
[28] Nowy S, Krummacher B C, Frischeisen J, Reinke N A and Brütting W 2008 *J. Appl. Phys.* **104** 123109
[29] Kim J B, Lee J H, Moon C K and Kim S Y 2013 *Adv. Mater.* **25** 3571
[30] Lee J H, Lee S H, Kim J B, Jang J H and Kim J J 2012 *J. Mater. Chem.* **22** 15262
[31] Nowy S 2010 Understanding losses in OLEDs: optical device simulation and electrical characterization using impedance spectroscopy *PhD Thesis* Universität Augsburg
[32] Palik E D 1997 *Handbook of Optical Constants of Solids* (San Diego, CA: Academic)